When precise numerical predictions come to the rescue of liquid lubrication

J.-D. Wheeler[1], V. Bruyere[1], P. Namy[1]
1. SIMTEC, 155 Cours Berriat, 38000 Grenoble, France

Introduction

Whereas solid mechanics can be considered as a well mastered science, the interface between the mating solids gathers several understanding difficulties. On the one hand, any observation attempt becomes a serious challenge as the solids inherently hide the object under investigation. On the other hand, the contact behaviour is generally ruled by multiphysic and multiscale phenomena. As a result, both experimental and numerical approaches are complex. It is often mandatory to use them both at the same time to complete their respective weaknesses.

The modelling of liquid lubrication is generally based on Reynolds equation [1] which is a lower dimension form of Navier-Stokes equations. Under some assumptions, the solution of this Reynolds equation has been obtained for the first time by Sommerfeld [2] in 1904 for journal bearings. This opened the way to the modelling of conformal contacts such as pad bearings, gas bearings and hydrostatic bearings. The lubrication regime of conformal contacts is known as the hydrodynamic regime. To analyse concentrated contacts, it is often mandatory to solve the solids deformations together with the Reynolds equation. In 1951 Petrusevich [3] achieved this goal for the first time and Dowson and Higginson [4] proposed formulae for line contacts that are still being used nowadays. Indeed, these formulae enable film thickness predictions for, among others, gears, deep groove ball bearings and roller bearings. When both elastic deformation and hydrodynamic effects are involved, the lubrication regime is referred to as the elastohydrodynamic (EHD) lubrication (EHL). For more details about the EHL modelling, refer to Lugt and Morales-Espejel [5].

In the present document, an overview of the phenomenon involved in EHL is presented through the typical case of the lubricated slider bearing. This industrial component will be described and the governing equations driving its behaviour will be presented. A solving method will then be proposed and validated. Then, the influence of the different physical phenomena on the slider lubrication will be discussed.

Theory

The slider bearing is a basic engineering component allowing to carry a load and limit the wear by a fluid film separation of the solids. Here, it is defined by its length, thickness and wedge (see **Figure 1**). The width of the slider is outside of the drawing plane.

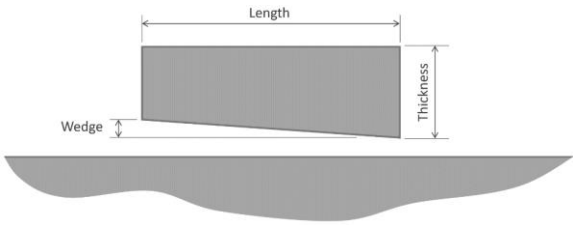

Figure 1. Slider bearing geometry

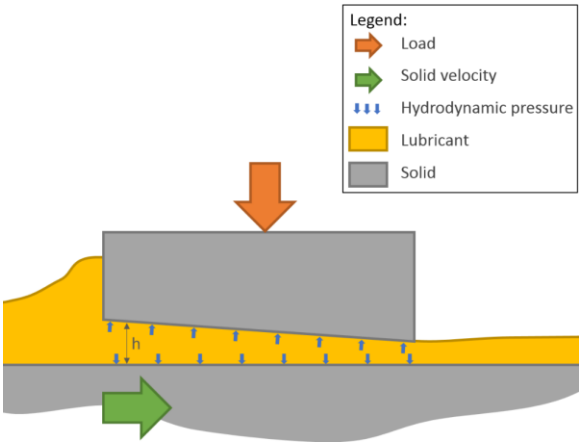

Figure 2. Slider bearing with its lubricant

Figure 3. Michell thrust block at the London Science Museum (By Andy Dingley - Own work, CC BY-SA 3.0, https://commons.wikimedia.org/w/index.php?curid=4944466)

Figure 2 presents the slider bearing with the two solids and the lubricant in between. The top solid is static ($u_t = 0\ m/s$), while the bottom solid is moving at the velocity u_b. A load w is applied on the top solid and it is transmitted to the bottom solid through the

hydrodynamic pressure in the lubricant. This pressure distribution is generated by the lubricant flow in the convergent shape of the top solid. The mean pressure under the solid is then $w/(width \cdot length)$.
This load carrying device is more generally used under its rotational forms: the thrust bearing (see **Figure 3**) and the tilting pad journal bearing (see **Figure 4**). However, for understanding purposes, the classical slider bearing is investigated.

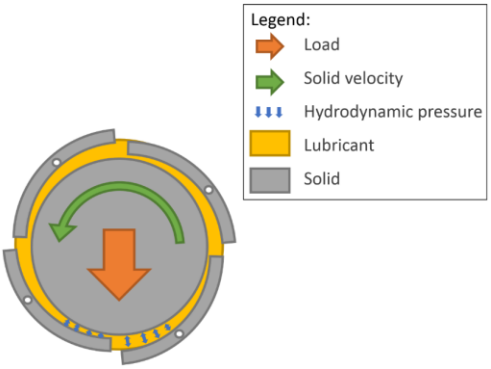

Figure 4. tilting pad journal bearing

Governing Equations

a) Reynolds equation [1]

By considering a thin film flow, the pressure is supposed to be constant across the film thickness. This enables efficient modelling of the lubricant film. The slider bearing is considered as infinitely wide, but the lineic load is chosen so that the mean pressure is the same as the real bearing. The Reynolds equation reads, in its one-dimension stationary form:

$$\frac{\partial}{\partial x}\left(\frac{\rho h^3}{12\eta}\frac{\partial p}{\partial x}\right) - u_e\frac{\partial(\rho h)}{\partial x} = 0$$

with x the space dimension along the slider length, ρ the lubricant density, h the film thickness, η the lubricant viscosity, p the hydrodynamic pressure $u_e = (u_t + u_b)/2$ the entrainment velocity, $u_t = 0\ m/s$ the top solid velocity and u_b the bottom solid velocity. At the extremities of this domain, a $p = 0$ boundary condition is applied (see **Figure 5**).

Figure 5. Reynolds domain and boundary conditions

b) Film thickness expression

The film thickness is expressed as follows:

$$h = h_0 + h_r(x) + v(x) + R(x)$$

with h_0 the distance between the rigid bodies, h_r the thickness of the rigid gap, v the solid deformation sum and R the surface texture.

c) Solids deformation

When the solids deformations are considered, the displacement field $\boldsymbol{u} = \{u, v\}$ is computed:

$$\boldsymbol{\nabla} \cdot \boldsymbol{\sigma} = 0$$

with $\boldsymbol{\sigma} = \boldsymbol{C}(E_{eq}, \nu_{eq}) \cdot \boldsymbol{\varepsilon}$, $\boldsymbol{\varepsilon} = \frac{1}{2}(\nabla \boldsymbol{u} + \nabla \boldsymbol{u}^T)$ and with E_{eq} and ν_{eq} as specified in the Appendix 1. The boundary conditions are defined as specified in **Figure 6**.

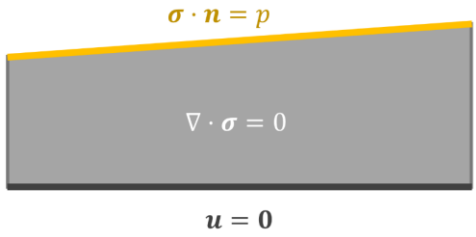

Figure 6. Solids deformation computation and boundary conditions

The solid deformation sum is not supposed to play a role as significant as in EHL point contacts, but it may change the gap shape of this conformal contact.

d) Load balance

As the slider load is carried by the hydrodynamic pressure, the load balance equation is verified:

$$w = \int_{Reynolds\ domain} p\ dx$$

with w the load applied on the slider. The variable determined by this equation is h_0. Indeed, the solids separation will highly influence the pressure distribution and in turn influence the load carrying capacity.

e) Heat transfer

Here a basic implementation of the thermal effects is proposed. In the solids, the heat equation is solved:

$$-\nabla \cdot k\nabla T = 0$$

with k the solids thermal conductivity (only valid for symmetric material bearings). Besides, the temperature is supposed to be constant across the lubricant film and equal to the solid mating surfaces, which are rough hypothesis. For quantitative predictions of thermal effects, the lubricant temperature should be free to vary in the thickness and the two solids should be represented. This would enable to consider the real kinematic influence on thermal effects (see Doki-Thonon et al.[6] for instance). However, the basic assumption selected here enables

a first approach. The heat transmitted to each solid (generated by the shearing in the lubricant) reads:

$$Q_s = h \cdot \eta \cdot \dot{\gamma}^2$$

with $\dot{\gamma} = |u_b - u_t|/h$ the shear rate. It intervenes as a boundary condition, as represented in **Figure 7**. The other boundary condition, at the bottom of the slider, accounts for a thermal regulation of the mechanism (see **Figure 7**), with T_0 the ambient temperature.

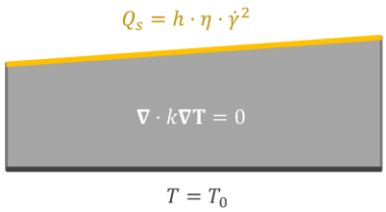

Figure 7. Heat transfer domain and boundary conditions

Constitutive relations

The constitutive relations proposed here are not restrictive and other possibilities are available. However, the present relations are relevant for the slider bearing case.

a) Compressibility

The density of the lubricant is predicted (unless otherwise specified) by the Dowson and Higginson [7] relation, together with a thermal expansivity term proposed by Ehret et al. [8]:

$$\rho(p,T) = \rho_0 \cdot \frac{5.9\ 10^8 + 1.34\ p}{5.9\ 10^8 + p} \cdot \left(1 - \beta \cdot (T - T_0)\right)$$

with ρ_0 the lubricant density at ambient temperature and pressure, β the thermal expansivity coefficient and T the lubricant temperature.

b) Piezoviscosity

In this model, a Roelands equation [9] is selected to account for the Newtonian viscosity temperature pressure relationship:

$$\mu(p,T) = \left(\mu_0\, e^{-\gamma\,(T-T_0)}\right) \left(\frac{\mu_0}{\mu_R}\right)^{\left(1+\frac{p}{p_R}\right)^{z-1}}$$

with μ_0 the viscosity at ambient pressure and temperature, γ the temperature viscosity coefficient, μ_R the reference viscosity, p_R the reference pressure, $z = \alpha\, p_R/\ln(\mu_0/\mu_R)$ the piezoviscosity index, and α the piezoviscosity coefficient. The first term corresponds to the temperature influence and the second one corresponds to the pressure influence.

c) Shear thinning

As the shear stress may exceed the Newtonian behaviour limit of the lubricant under some operating conditions, a shear thinning equation is also included in the model. This Carreau-Yasuda [10] expression reads:

$$\eta(p,T,\tau) = \frac{\mu(p,T)}{\left(1 + \left(\frac{\tau}{G}\right)^a\right)^{\frac{\frac{1}{n}-1}{a}}}$$

with $\tau = \mu\,\dot{\gamma}$ the shear stress, G, a and n parameters of the Carreau-Yasuda expression.

Solving method

The method used here is composed of two steps. The first one is an initialisation step, where solid deformation, temperature variations and shear stress influence are not included. At this stage:

$$v(x) = 0$$
$$T = T_0$$
$$\tau = 0$$

A second step is included if necessary, to solve the effects selected in the computation case (such as heat equation or solid deformations) and not accounted for in the initialisation step.

Results and discussion

In this work, an application was developed to configure the computation cases and to obtain the postprocessing results easily. The operating conditions selected for the study are in **Table 1** and the lubricant and solid properties are in **Table 2**. Both operating conditions and material properties are representative of industrial cases. Depending on the case investigated, these properties and operating conditions are modified accordingly to the case description.

Parameter	Value [unit]
u_t	10 $[m/s]$
w	40 000 $[N]$
Width	50 $[mm]$
Length	60 $[mm]$
Thickness	10 $[mm]$
Wedge	10 $[\mu m]$

Table 1. Reference case operating conditions

	Parameter	Value	Unit
Density parameters	ρ_0	900	kg/m^3
	β	$6.4 \cdot 10^{-4}$	K^{-1}
	T_0	293.15	K
Newtonian viscosity parameters (from Ehret et al.[8])	μ_0	0.04	$Pa \cdot s$
	α	$15 \cdot 10^{-9}$	Pa^{-1}
	γ	0.042	K^{-1}
	μ_R	$6.4 \cdot 10^{-4}$	$Pa \cdot s$
	p_R	196	MPa
Non-Newtonian parameters	G	20	kPa
	n	0.35	–
	a	5	–
Surfaces	Perfectly smooth		
Solids	E_t, E_b	$2.1 \cdot 10^{11}$	Pa
	ν_t, ν_b	0.3	–

Table 2. Lubricant and solid properties

a) Isoviscous and incompressible fluid

The lubricant properties are here independent of pressure, temperature or shear stress. Moreover, the solids are rigid. Under these lubricant and solid assumptions, it is possible to derive an analytical solution (see Hamrock, Schmid and Jacobson[11]) to the plane slider bearing case. The results of this analytical model are plotted together with the numerical model results in **Figure 8**. The analytical solution can only provide a pressure distribution based on a given distance between the rigid bodies h_0, so a simple routine was used so that the load carrying capacity matches the load of the numerical case. The authors would like to specify that this is not a fitting routine as the analytical result is obtained independently from the numerical result.

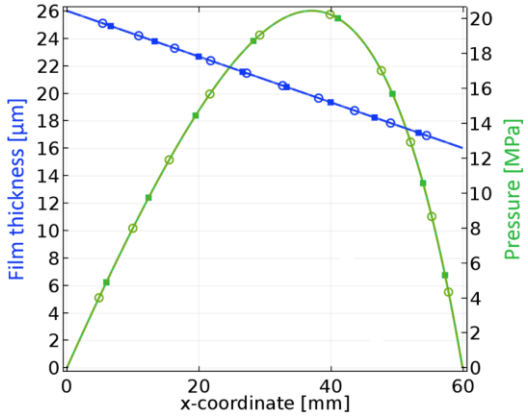

Figure 8. Film thickness and pressure - comparison between analytical (··o··) and numerical (—▪—) results

Analytical and numerical results are in good agreement (relative difference $< 2 \cdot 10^{-6}$ % for both pressure and film thickness) and it validates the numerical precision under isoviscous and incompressible lubricant assumptions.

Real life lubricants are more complex, and their behaviour must be accounted for to quantitatively predict the bearing life span or efficiency. Apart from the lubricant rheology, the thermal effects also have a significant role. It also important to notice that solids are neither smooth nor rigid: solid elasticity and surface roughness will be investigated. Moreover, this slider geometry is only one of the possible geometries.

b) Piezoviscous and compressible fluid (**reference case**)

Pressure influences viscosity and density. This influence often plays a significant role, especially at high hydrodynamic pressure. Here this influence is included, but the lubricant is still Newtonian and isothermal, and the solids are rigid.

The present case will be considered as the reference case in the followings.

Figure 9 shows that neglecting pressure dependence of viscosity and density (as in a) Isoviscous and incompressible fluid) leads here to underestimating the minimum film thickness by $1\ \mu m$ and the maximum pressure by $1\ MPa$.

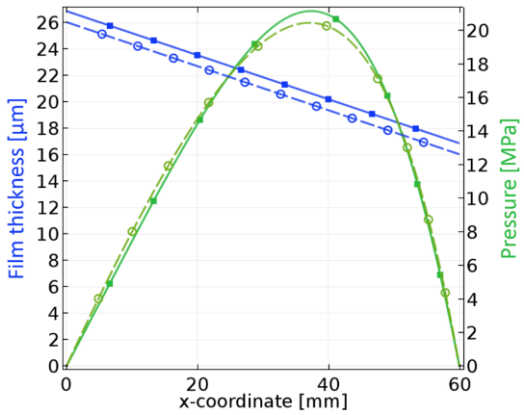

Figure 9. Film thickness and pressure – comparison between reference case (—▪—) and the isoviscous and incompressible analytical solution (- - o - -)

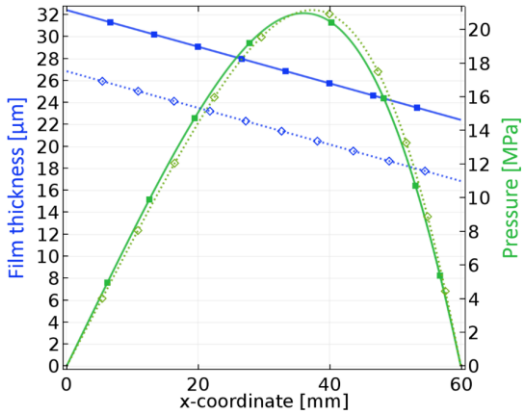

Figure 10. Film thickness and pressure – comparison between reference case (··◊··) and reference case with $u_b = 20\ m/s$ (—▪—)

c) Velocity

The velocity plays a significant role on the bearing behaviour. The present case is like the reference case apart from the velocity ($u_b = 20\ m/s$) and its influence is presented in **Figure 10**. Here, the minimum film thickness increased by about $5\ \mu m$ comparing to the reference case, because of the velocity rise. The pressure distribution is hardly affected. However, the real influence of velocity can only be analysed with a temperature and shear stress dependant lubricant model. Indeed, the shearing energy dissipated in the lubricant film is $\propto w \cdot (u_t - u_b)^2$, and a shear rate increase leads to a large heat increase, a viscosity decrease and a resulting film thickness drop.

d) Load

The reference case is computed with a load of $w = 80000\ N$. **Figure 11** presents the film thickness which is reduced comparing to the reference case film. As expected, the pressure is larger than the one of the reference case.

Similarly to the increased velocity case, the actual behaviour of the bearing under high loads can only be predicted with more complex lubricant models than the one used in the present case.

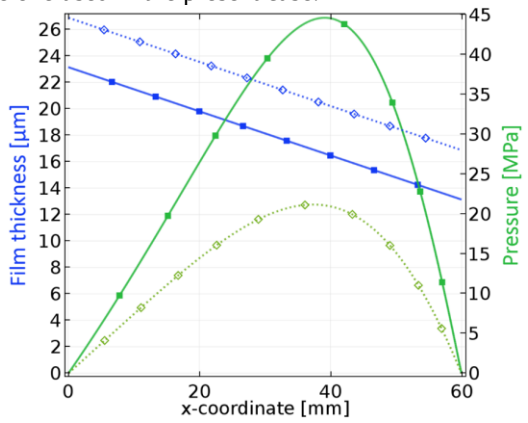

Figure 11. Film thickness and pressure – comparison between reference case (··◊··) and reference case with $w = 80000\ N$ (—▪—)

e) Thermal effects

As mentioned previously, thermal effects have a significant influence on the contact at large load and large velocity. Consequently, a severe reference case is defined, with $u_b = 20\ m/s$ and $w = 80000\ N$. The other operating conditions and hypothesis are the same as the reference case. In **Figure 12**, the results of this severe reference case are compared with the results of the same case, but with the thermal effects included (obtained by heat equation computation fully coupled with Reynolds equation).

Whereas the pressure distribution is lightly affected by the thermal effects, the minimum film thickness is divided by two when the thermal effects are included. This means that neglecting them leads to a significant overestimation of film thickness and therefore to the dramatic underestimation of wear and lifespan.

f) Non-Newtonian lubricant

Under high shearing conditions, the lubricant may exhibit a shear thinning behaviour. This means that the viscosity is reduced by the shear stress, which leads to a film thickness reduction (similarly to the thermal effects). In **Figure 13**, the severe reference case results are compared with the severe reference case results with the non-Newtonian effects included.

Figure 13 shows that the shear thinning leads here to a film thickness reduction of about $4\ \mu m$. Again, neglecting the shear thinning behaviour may lead to hazardous predictions of the minimum film thickness.

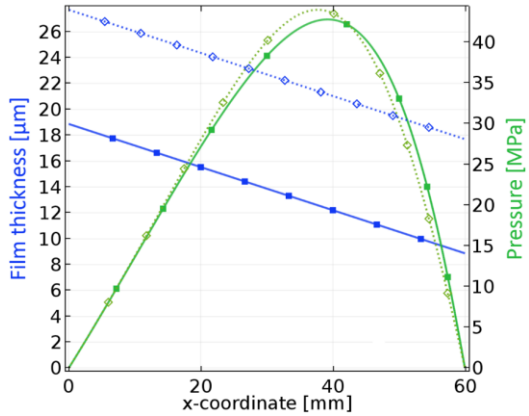

Figure 12. Film thickness and pressure – comparison between severe reference case with (—▪—) and without (··◊··) thermal effects

g) Solid deformation

When large pressures are encountered, the elastic properties of the solids cannot be neglected anymore. It is EHL. Indeed, the large pressures deform the slider gap and the fluid flow will be modified. Both the slider and the track are made of steel, with $E_t = E_b = 210\ GPa$ and $\nu_t = \nu_b = 0.3$.

In **Figure 14**, the solid deformation sum is computed for the severe reference case, and its influence on pressure and film thickness is highlighted. Here, the pressure distribution is more asymmetrical with the solids deformation included than without them. Besides, the minimum film thickness is reduced by the solids deformations. This shows that under certain conditions, the solids deformation should be included for accurate film thickness predictions.

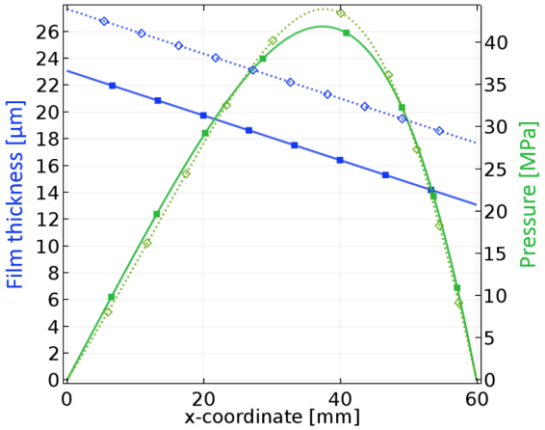

Figure 13. Film thickness and pressure – comparison between severe reference case with (—▪—) and without (··◊··) non-Newtonian behaviour

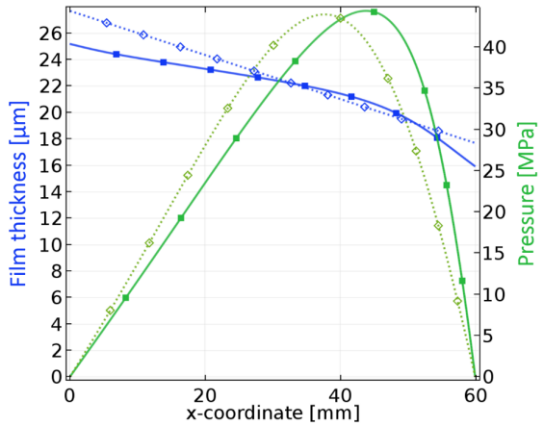

Figure 14. Film thickness and pressure – comparison between severe reference case with (—▪—) and without (··◊··) solid deformations included in the film thickness expression

h) Surface texture

Whereas smooth surfaces do not exist in real life, it is sometimes difficult to take them into account in tribology models. Indeed, their geometries are generally at a smaller scale than the contact width or length. The roughness is either desired (to trap wear particles, retain lubricant, improve lubricant replenishment) or undesired (often a result of the manufacturing process) as they reduce the minimum film thickness. A first approach is to add a sine function $R(x) = A_0 \cdot \sin(B_0 x)$ to the film thickness expression. In the present stationary reference case computation, it means that the roughness is added to the top solid which velocity is nought.

The results are presented in **Figure 15**, and the minimum film thickness is noticeably reduced by the roughness presence. The pressure is locally increased. This comparison shows that under certain conditions they should be included in the model.

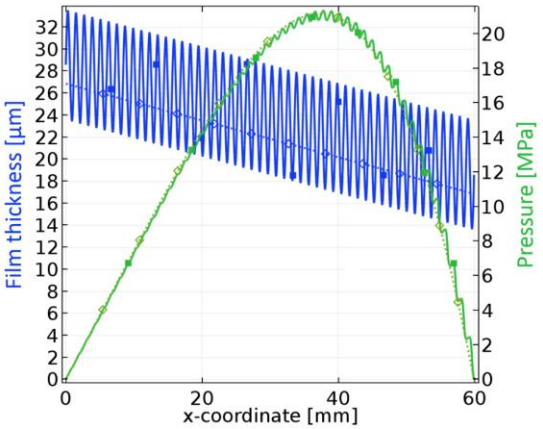

Figure 15. Film thickness and pressure - comparison between reference case with (—▪—) and without sine texture (··◊··) under the reference case operating conditions

i) Slider geometry

The slider geometry can be different. Instead of a plane slider bearing, the slider can be separated into an inclined plane together with a horizontal plane. This geometry limits the contact pressure at nought velocity (only dry contact pressure). This slider gap is presented in **Erreur ! Source du renvoi introuvable.**. T he minimum film thickness is very similar to the one of the reference case, but the maximum pressure is slightly larger. The pressure distribution is also more symmetrical than the one of the reference case.

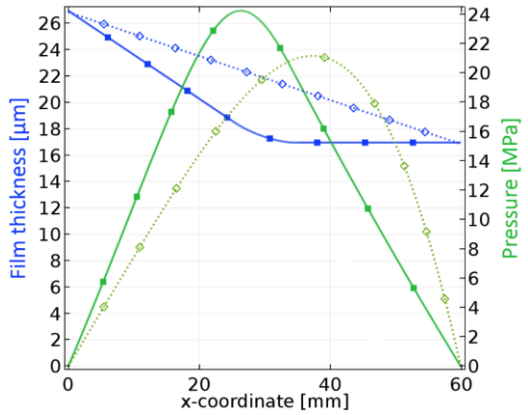

Figure 16. Film thickness and pressure – comparison between two planes slider bearing (—▪—) and plane slider bearing (··◊··) under the reference case operating conditions

Another solution to limit the contact pressure at nought velocity is the Rayleigh step bearing. The gap defined by the step bearing is defined in **Figure 17**.

With the step bearing and in the reference case conditions, the maximum pressure is larger than the one of the plane bearing. The pressure distribution is also more symmetrical.

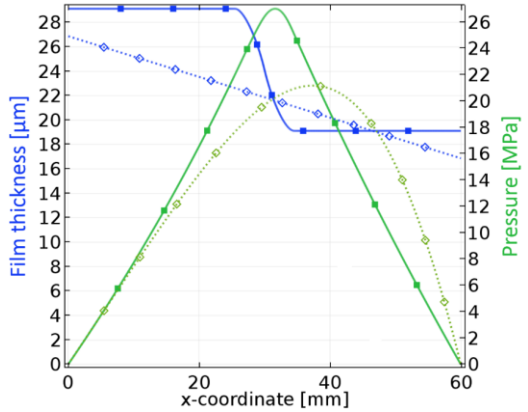

Figure 17. Film thickness and pressure – comparison between plane slider (—▪—) and Rayleigh step bearing (··◊··) under the reference case operating conditions

Conclusions

Even if the contact understanding is a challenge, an appropriate modelling of the different phenomena allows for overcoming it. In the present document, the most common effects have been shortly presented and the main prediction mistakes attached have been introduced. The different cases computed show the great influence of each of the different effects. Selecting the ones to neglect and the ones to include is a difficult task.

The present model does not propose new hypothesis but aims to demonstrate the existing challenges in EHL. To optimise the workflow a COMSOL Application was developed together with this model and COMSOL Server with an https secured connexion was used to solve the different cases on a distant high-performance computer.

References

1. Reynolds, O. On the Theory of Lubrication and its Application to Mr. Beauchamp Tower's Experiments, including an Experimental Determination of the Viscosity of Olive Oil. *Trans. ASME* (1886).
2. Sommerfeld, A. Zur hydrodynamischen theorie der schmiermittelreibung. *Zeit. Math. Phys., Bd* **50,** 97 (1904).
3. Petrusevich, A. I. Fundamental conclusions from the contact-hydrodynamic theory of lubrication. *Izv. Akad. Nauk SSSR* **3(2),** 209–223 (1951).
4. Dowson, D. & Higginson, G. R. A numerical solution to the elasto-hydrodynamic problem. *J. Mech. Eng. Sci.* **1,** 6–15 (1959).
5. Lugt, P. M. & Morales-Espejel, G. E. A review of Elasto-hydrodynamic lubrication theory. *Tribol. Trans.* **54,** 470–496 (2011).
6. Doki-Thonon, T., Fillot, N., Vergne, P. & Morales-Espejel, G. E. Numerical insight into heat transfer and power losses in spinning EHD non-Newtonian point contacts. *J. Eng. Tribol.* **226,** 23–35 (2012).
7. Dowson, D. & Higginson, G. R. *Elastohydrodynamic lubrication, the fundamentals of roller and gear lubrication*. (1966).
8. Ehret, P., Dowson, D. & Taylor, C. M. Thermal Effects in Elliptical Contacts with Spin Conditions. in *Proceedings of the 25th Leeds-Lyon Symposium on Tribology* **36,** 685–703 (Elsevier, 1999).
9. Roelands, C. Correlational aspects of the viscosity-temperature-pressure relationship of lubricating oils. (Delft University (V. R. B. Groningen) The Netherlands, 1966).
10. Bair, S. A Rough Shear-Thinning Correction For EHD Film Thickness. *Tribol. Trans.* **47,** 361–365 (2004).
11. Hamrock, B. J., Schmid, S. R. & Jacobson, B. O. *Fundamentals of Fluid Film Lubrication*. (2004).
12. Habchi, W., Eyheramendy, D., Vergne, P. & Morales-Espejel, G. E. A full-system approach to the elastohydrodynamic line/point contact problem. *J. Tribol.* **130(2),** 21501–21510 (2008).
13. Habchi, W. A full-system finite element approach to elastohydrodynamic lubrication problems: application to ultra-low-viscosity fluids. (Institut National des Sciences Appliquées de Lyon, INSA, 2008). doi:2008ISAL0038

Appendix: Equivalent solid

It is a common choice in the EHD domain to apply the equivalent body theory (see [12,13]). As a result, only one body must be modelled. The equivalent Young modulus and Poisson ration are expressed as follows:

$$E_{eq} = \frac{E_b^2 E_t (1+\nu_t)^2 + E_t^2 E_b (1+\nu_b)^2}{\left(E_b(1+\nu_t) + E_t(1+\nu_b)\right)^2}$$

$$\nu_{eq} = \frac{E_b \nu_t (1+\nu_t) + E_t \nu_b (1+\nu_b)}{E_b(1+\nu_t) + E_t(1+\nu_b)}$$

with E_b and E_t respectively the Young modulus of the bottom and top solid, and ν_b and ν_t the bottom and top Poisson ratio.